

See discussions, stats, and author profiles for this publication at: <https://www.researchgate.net/publication/51732335>

Diffraction light trapping in crystal-silicon films: Experiment and electromagnetic modeling

Article in *Applied Optics* · October 2011

DOI: 10.1364/AO.50.005728 · Source: PubMed

CITATIONS

2

READS

65

7 authors, including:



Dirk Weiss

University of Washington Seattle

12 PUBLICATIONS 335 CITATIONS

[SEE PROFILE](#)



Benjamin G Lee

Hanwha Q CELLS

78 PUBLICATIONS 1,337 CITATIONS

[SEE PROFILE](#)



William Nemeth

Battelle Memorial Institute

60 PUBLICATIONS 596 CITATIONS

[SEE PROFILE](#)



qi Wang

St. Andrews University

84 PUBLICATIONS 2,509 CITATIONS

[SEE PROFILE](#)

Some of the authors of this publication are also working on these related projects:



Silicon Epitaxy [View project](#)



Si related work [View project](#)

Diffractive light trapping in crystal-silicon films: experiment and electromagnetic modeling

Dirk N. Weiss,^{1,*} Benjamin G. Lee,² Dustin A. Richmond,¹ William Nemeth,² Qi Wang,² Douglas A. Keszler,³ and Howard M. Branz²

¹Washington Technology Center and University of Washington, Department of Electrical Engineering, Seattle, Washington 98195, USA

²National Renewable Energy Laboratory, 1617 Cole Blvd., Golden, Colorado 80401, USA

³Department of Chemistry, Oregon State University, 153 Gilbert Hall, Corvallis, Oregon 97331, USA

*Corresponding author: dnweiss@uw.edu

Received 11 April 2011; revised 23 August 2011; accepted 25 August 2011;
posted 26 August 2011 (Doc. ID 145693); published 6 October 2011

Diffractive light trapping in $1.5\text{ }\mu\text{m}$ thick crystal silicon films is studied experimentally through hemispherical reflection measurements and theoretically through rigorous coupled-wave analysis modeling. The gratings were fabricated by nanoimprinting of dielectric precursor films. The model data, which match the experimental results well without the use of any fitting parameters, are used to extract the light trapping efficiency. Diffractive light trapping is studied as a function of incidence angle, and an enhancement of light absorption is found for incidence angles up to 50° for both TE and TM polarizations. © 2011 Optical Society of America
OCIS codes: 050.0050, 310.6845.

1. Introduction

Thin crystal silicon (c-Si) solar cells, with a silicon thickness range of $2\text{--}20\text{ }\mu\text{m}$, hold the promise to combine the high conversion efficiencies of silicon wafer technology with the scalability and cost effectiveness of thin-film technologies. Poor absorption of near-bandgap light in c-Si, however, is a central issue to be solved with this emerging technology [1–6]. Diffractive grating couplers at both the front [7–11] and back sides [1,3,5,12–18] of thin-film silicon solar cells have been proposed and tested to assess their light-trapping potential for poorly absorbed wavelength ranges in the red and near-IR parts of the solar spectrum. It is evident that, at certain wavelengths, grating couplers can greatly outperform the more commonly used random scatterers because 100% of the light can be trapped through waveguiding [12]. However, the relatively broad solar

spectrum, the varying angle of incidence in a non-tracking solar cell, and the largely unpolarized nature of sunlight contribute to losses that may render diffractive light trapping less effective. Hence, the question whether diffractive couplers can, in a practical realization, outperform random, so-called Lambertian scatterers is yet to be answered.

We recently published a nanoimprint method for dielectric materials [19] and measured its light-trapping performance on $25\text{ }\mu\text{m}$ thick silicon wafers [5]. We believe this nanoimprint technique addresses the cost-effective fabrication of grating structures with well-defined, subwavelength features covering the whole solar cell area. Moreover, our technique does not require etching a grating into the cell itself, and it can be applied as a final step before encapsulation of finished cells. Thus, the method is easy to implement and does not degrade cell performance. In this paper, we present our first results for diffractive light trapping in far thinner c-Si film devices in both glass “superstrate” and “substrate” configurations. Light trapping is analyzed by combining

measurement and theory. We performed hemispherical reflection measurements and then modeled both the hemispherical reflection and the light absorption in the silicon layer with the rigorous coupled-wave analysis (RCWA) method. The light absorption in the silicon, extracted from the reflection model, enables the calculation of the expected short-circuit current increase due to light trapping. We further studied, both experimentally and through RCWA modeling, the effect of the incidence angle on diffractive light trapping in a superstrate film stack, for both TE and TM polarizations. Although the angular dependence of diffractive light trapping has been addressed in the literature [18], we believe that our contribution is the first experimental and theoretical proof that grating back reflectors provide enhancements of short-circuit current vis-à-vis flat back reflectors at incidence angles greater than 0° . Using simulations, we highlight the role of diffraction efficiencies on light trapping. Finally, we show experimental results for two different gratings in substrate configuration.

2. Experimental and Modeling Details

Hydrogenated amorphous Si films were deposited on Corning Eagle glass substrates by plasma-enhanced chemical vapor deposition (PECVD). The films were then oven-crystallized in two steps in a nitrogen environment. An initial 1 h anneal at 450°C effused most hydrogen from the film, and a 15 h anneal at 650°C crystallized the Si to grains about $1\ \mu\text{m}$ in diameter. The temperature was ramped at $5^\circ\text{C}/\text{min}$ [20]. For the superstrate samples, we applied a dielectric diffraction grating and silver reflector film directly to the Si film and admitted light from the glass side [Fig. 1(a)]. For the substrate samples, we applied a 122 nm thick PECVD silicon nitride film as a quarter-wavelength antireflection coating after Si crystallization. For these samples, we applied the diffraction grating and silver reflector film to the glass side and light was incident from the silicon-nitride side. Both c-Si and nitride thickness were measured by reflectance and transmission with an n&k 1700RT analyzer.

The transparent, dielectric grating films were fabricated by spin coating aluminum oxide phosphate precursor and subsequent thermal nanoimprinting using ethylene tetrafluoroethylene molds, as described previously [5,19], except for the following changes: the precursor concentration was reduced by a factor of 2, the imprint temperature was increased to 180°C , and the postimprint annealing temperature was increased to 500°C . These changes enabled the fabrication of thinner films with a more homogeneous thickness. The higher annealing temperature provided an almost complete elimination of water and acid from the dielectric film, and 100 nm thick silver reflector films were deposited onto the gratings by electron-beam evaporation using a planetary substrate holder.

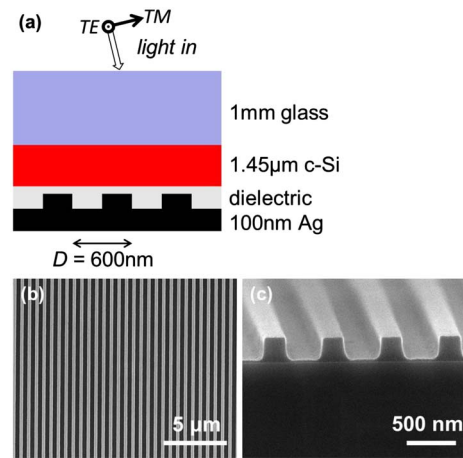


Fig. 1. (Color online) (a) Schematic of crystal-Si film on glass superstrate, with imprinted dielectric grating and silver reflector. The directions of the electric field vector for TE and TM polarized light are indicated. (b) SEM micrograph of 600 nm imprinted dielectric grating on Si wafer substrate, without metal reflector, top view. The grating has a period of 600 nm and a grating height and average width of both 225 ± 5 nm; the residual layer, defined as the continuous layer between the grating valley and the substrate/dielectric interface, is 30 ± 2 nm thick. (c) As (b), 88° side view.

Imprint topography was imaged with scanning electron microscopy (SEM) using an FEI Sirion microscope with 5 kV acceleration voltage and through-lens detector. To avoid sample charging problems, dielectric gratings identical to the ones used for the film devices were fabricated on Si wafers instead of Si film/glass stacks and AuPd alloy films 5 nm thick were sputter coated onto the imprinted and annealed dielectric layers prior to SEM imaging.

Hemispherical reflection measurements were performed in TE and TM polarizations using a Varian Cary 6000i UV/Vis/NIR spectrometer with integrating sphere (DRA-1800). The light was linearly polarized, with the E-vector (H-vector) parallel to the grating lines for TE (TM) polarization. The grating samples were always oriented such that the grating lines were perpendicular to the plane of incidence in order to obtain unmixed TE and TM polarizations (the plane of incidence is defined by incident beam and surface normal directions) [5]. In addition, the incidence angle for illumination was varied using a clip-style variable-angle center-mount holder.

Electromagnetic modeling was performed for the technologically more relevant superstrate sample geometry with the RCWA method for square grating reflectors using the DiffractMod software package (RSoft Design Group, Inc., Ossining, New York). We present and discuss the following model outputs: the total reflection, which can be directly compared to the experimental hemispherical reflection; the light absorbed in the Si layer, which is obtained using the RSoft Monitor function; and the diffraction efficiencies for a particular grating. TE or TM polarized light at varying incidence angles with respect to the surface normal were studied separately. The

experimental n and k values were used for the nanoimprinted dielectric film material, aluminum oxide phosphate [5,21]. The n and k values for c-Si from the compilation by Aspnes were used [22]. For the analysis of diffraction efficiencies, the incident light wave was launched inside the Si layer, and the Si optical constants were replaced by those of a nonabsorbing dielectric with $n = 3.5$. Glass was modeled with wavelength-independent $n = 1.5$ and $k = 0$. Silver was modeled with the optical constants provided by RSoft.

3. Results and Discussion

Figure 1 shows the schematic of the investigated stack in superstrate configuration, along with SEM micrographs of a 600 nm period imprinted dielectric grating on c-Si. The defect-free grating has an area

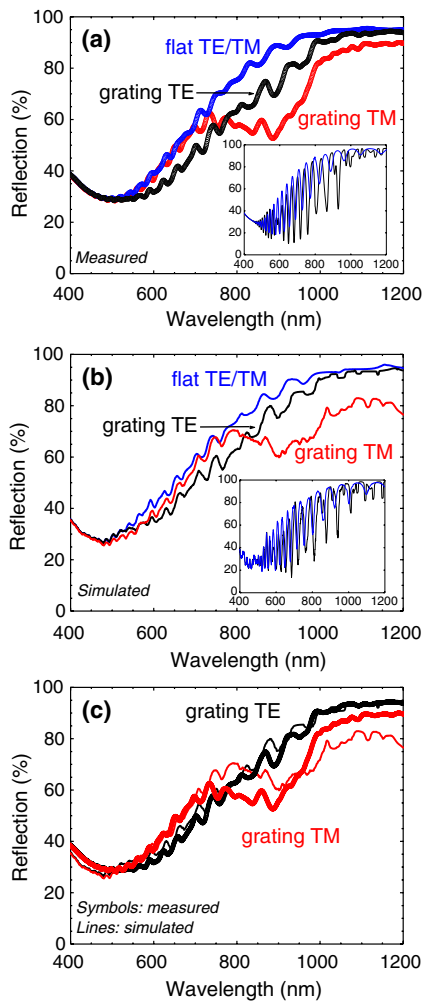


Fig. 2. (Color online) (a) Experimental hemispherical reflection data for a 1.45 c-Si film on glass superstrate, with grating and flat reference reflector, TE and TM polarizations, 8° incidence angle (averaged data). Inset: raw data for grating (black curve) and flat (blue curve) reflector, TE polarization only. (b) Simulated data using RCWA method, for grating and flat reflectors, 8° incidence angle (averaged data). Inset: raw data for grating (black curve) and flat (blue curve) reflector, TE polarization only. (c) Comparison of experimental and simulated data for gratings, TE and TM polarizations.

of 64 mm². Figure 2(a) shows the experimental reflection data for the 1.45 μm thick c-Si superstrate stack. The interference fringes are smoothed using a ±50 nm window moving average, which preserves the area under the curves [3]. The averaging of both experimental and model curves enables a better visual comparison. The overall increase in reflection above 550 nm wavelength observed in all curves is due to increased transmission of light through the Si and subsequent reflection off the respective back reflectors. The transmission through the 100 nm Ag back reflector is negligible, meaning the total absorption $A(\lambda)$ in the stack can be calculated from the hemispherical reflection $R(\lambda)$ as $A(\lambda) = 1 - R(\lambda)$. The redshifted onset of reflection for the grating reflector indicates increased total light absorption in the stack [5,23]. We note that, for TM polarization, the shift of the reflection slope is only observed above 750 nm.

The total light absorption in the stack is the sum of absorption in the Si $A_s(\lambda)$ and parasitic absorption $A_p(\lambda)$ in the back reflector. $A_s(\lambda)$ cannot be obtained in a direct way from the optical measurements, so we extract it instead through electromagnetic modeling using the RCWA model. In Fig. 2(b), we plot the model curves for $R(\lambda)$ for the same stack, which show very good overall agreement with the experimental data [as shown in direct comparison for the grating curves in Fig. 2(c)]. The model contains no free fitting parameters, and the experimental geometric grating parameters noted in the caption of Fig. 1 were used. $A_s(\lambda)$ is extracted from this model and plotted for the flat and grating reflectors in Fig. 3(a). Increased absorption with respect to the flat reference reflector is observed for both grating curves. It is important to note that the peak absorption at 70% is so low because we have no antireflection coating between the glass and Si, nor on the glass front. In a practical solar cell design with appropriate antireflection coating(s), nearly 100% absorption can be easily achieved, at least in the 400–450 nm range. However, the focus of the present work is rather the relative improvement that can be achieved through diffractive light trapping. To obtain the effect of light trapping on the short-circuit current J_{sc} (mA/cm²) under solar illumination, $A_s(\lambda)$ must be weighed with the solar spectrum, which is computed from the following integral:

$$J_{sc} = e \int_{350 \text{ nm}}^{1100 \text{ nm}} A_s(\lambda) \Phi(\lambda) d\lambda, \quad (1)$$

where the solar photon flux $\Phi(\lambda)$ (photons/nm cm² sec) is derived from the AM 1.5 reference spectrum [24], and e is the elementary charge. The internal quantum efficiency is arbitrarily set to 1 (this factor does not influence the relative improvements due to light trapping that are object of this investigation). Figure 3(b) shows both the AM 1.5 solar photon flux curve $\Phi(\lambda)$, along with the integral (gray area) for the grating reflector and TE polarization. From the absorption curves in Fig. 3(a), we obtain

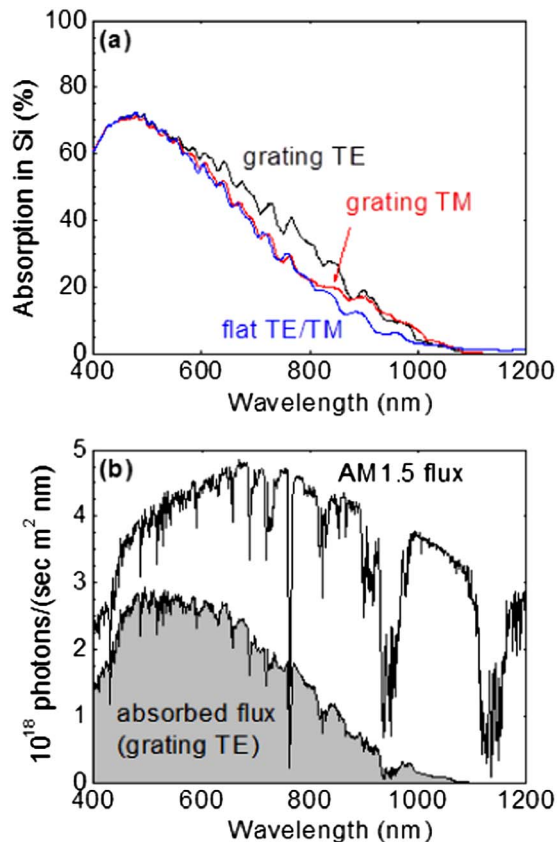


Fig. 3. (Color online) (a) Light absorption in the Si layer for grating and flat reflectors from the simulation in Fig. 2(b). (b) Terrestrial standard AM 1.5G solar photon flux and absorbed photon flux (gray area under curve, example for grating reflector, TE polarization). Absorption is less than 100% at all wavelengths because of reflective losses at the glass surface and the glass/Si interface.

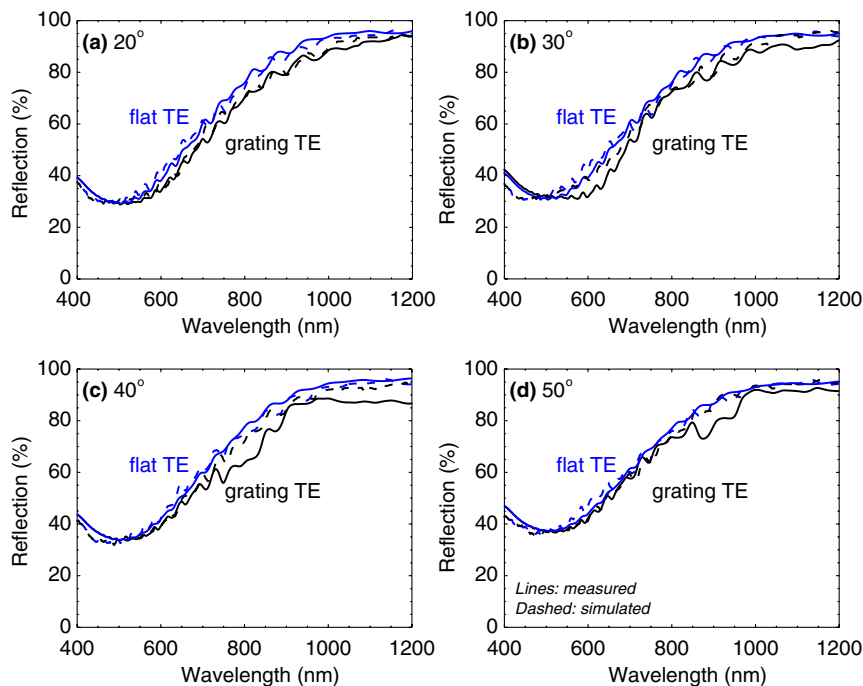


Fig. 4. (Color online) Experimental (solid curves) and simulated (dashed curves) hemispherical reflection data for the film in Fig. 2 for different incidence angles, to surface normal (averaged data, TE polarization only): (a) 20°, (b) 30°, (c) 40°, (d) 50°.

$J_{sc} = 17.22$ and 15.74 mA/cm² for the grating reflector for TE and TM, respectively, and $J_{sc} = 15.15$ and 15.21 mA/cm² for the flat reflector for TE and TM, respectively. Thus, the relative improvement in current density due to the grating is 13.6% and 3.5% for the TE and TM cases, respectively, and the increase for average polarization is 8.5%. As noted previously, the overall low values for J_{sc} originate in the lack of antireflection coating(s), which would be included in a practical solar cell design. Poor performance for TM polarization is likely exaggerated by the model, which predicts higher reflection (and, therefore, lower total absorption) than the experiment in the wavelength range 700–900 nm [Fig. 2(c)]. In the following paragraphs, we discuss the origin of the lower degree of light trapping in TM in the context of first-order diffraction efficiencies.

We next discuss the influence of the incidence angle on diffractive light trapping. Figure 4 shows the experimental and simulated reflection curves for the stack for four different incidence angles in TE polarization. The general trend observed is that the red-shift of the grating curves diminishes with increasing incidence angle. Only the wavelength ranges around 800 nm for 40° and around 900 nm for 50° incidence angle are exceptions to this observation. At these wavelengths, the model also shows higher reflectance values for the grating curves, which may result in an underestimation of the actual degree of light trapping in the experiment. At this point, we emphasize again that absorption losses in the grating reflector (both intrinsic and plasmonic) contribute to the total measured reflection and that no direct conclusion on nonparasitic light absorption in the

silicon can be drawn from the experiment. We extract the Si absorption from the simulated curves, as described earlier, and calculate the expected increase in J_{sc} due to diffractive light trapping. Figure 5 shows the results in terms of relative improvement in short-circuit current density for different incidence angles, for TE and TM polarizations, and the average of these. Although the improvement for average polarization decreases from 8.5% (8° incidence angle) to 3.4% (50° incidence angle), diffractive light trapping is observed in the entire angular range we investigated. We believe that this is the first quantitative evaluation of diffractive light trapping at varying incidence angles, although indirect evidence for light trapping non-normal incidence was recently published by the Neuchâtel group [18].

Light trapping in the stack is low compared to the ideal Lambertian light trapping limit [23,25]. While our grating obtained an 8.5% relative enhancement in solar photon absorption (and short-circuit current) compared to the flat reflector, a Lambertian reflector would lead to a 66% improvement. The latter value is calculated with a (noncoherent) ray-tracing model from our earlier work [5], which is based on the model by Deckman *et al.* [25], assuming a back reflector with 95% wavelength-independent reflectivity and Fresnel transmission through the glass/Si interface. The physical reason for our low light trapping efficiencies is likely the relatively weak diffraction of light at the particular grating reflector studied here. The simulated diffraction efficiencies in Fig. 6 show that only 15% to 18% of light is diffracted into nonzero orders in the wavelength range above 700 nm for TE polarization. For TM, the diffracted intensity is approximately zero at 800 nm and increases to about 70% with increasing wavelength. Dedicated reflection gratings in air, as used for spectroscopy, routinely achieve diffraction efficiencies of nearly 100% for certain wavelength ranges. In our case, the grating is clad with dielectric, and the Si layer is sufficiently close to the metal reflector to influence the diffraction intensities. Future work will focus on the role of both the dielectric environment

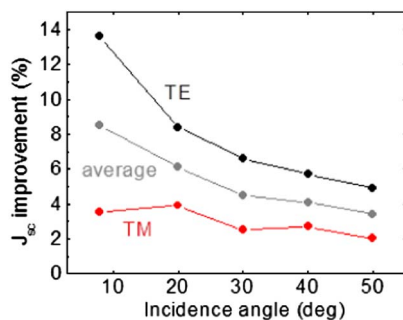


Fig. 5. (Color online) Improvement factors for the simulated short-circuit current density due to the grating reflector versus flat reflector for a 1.45 μm Si film device. TE and TM polarizations and the polarization-averaged improvement factors are shown (lines are a guide for the eye).

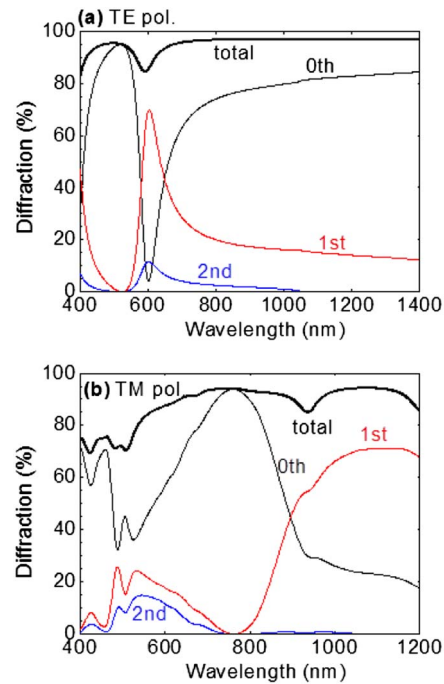


Fig. 6. (Color online) Simulated diffraction efficiencies for grating reflector: (a) TE polarization and (b) TM polarization (RCWA). First- and second-order diffraction efficiencies contain both $\pm 1\text{st}$ and $\pm 2\text{nd}$ orders. The third order is too weak to be displayed on this scale. The sum of all total diffraction efficiencies (curve marked “total”) is identical to the reflectivity of the interface. The light wave is launched inside the Si layer, with an incidence angle of 0°.

and the potential for grating optimization, both through experiment and simulations.

We note that the degree of light trapping, as seen in the redshift of reflection (Fig. 2), closely follows the first-order diffraction efficiency for both TE and TM as simulated in Fig. 6. The redshift for TE light is seen above 600 nm and a larger shift is seen above 800 nm for the TM case. This clearly demonstrates that the goal of grating design must be to diffract a maximum fraction of incident light intensity into the diffracted orders that can be absorbed in the film.

Up to this point we have discussed light trapping in the superstrate geometry, in which incident light first passes through a transparent glass plate. We finally present in Fig. 7 experimental data for two c-Si films with different dielectric grating reflectors in substrate geometry, in which the gratings are imprinted on the backsides of the glass substrates as schematically shown in the inset. These substrate films are measured with light incident on the silicon-nitride antireflection coating. We do not analyze these substrate results with the RCWA method as we did for the technologically more important superstrate data above, but we rather present these results to highlight the similarity of diffractive light trapping in different sample geometries. The 606 nm period grating in Fig. 7(a) shows light trapping comparable to the superstrate grating of the approximately same period discussed above [Fig. 2(a)],

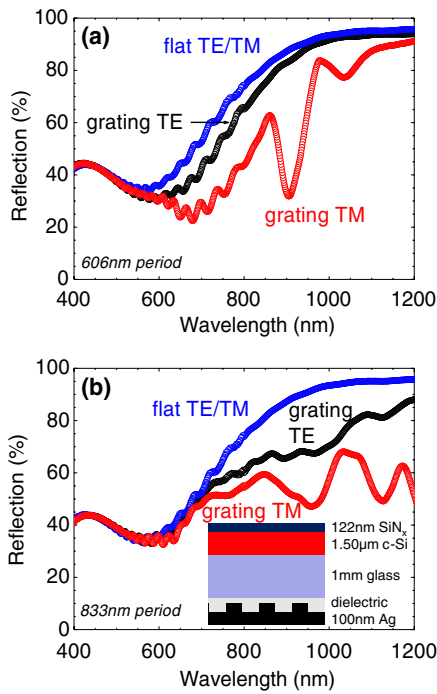


Fig. 7. (Color online) Experimental hemispherical reflection data for $1.50 \pm 0.05 \mu\text{m}$ c-Si films in substrate geometry, with grating and flat reference reflectors, TE and TM polarizations, 8° incidence angle. (a) 606 nm grating period, (b) 833 nm grating period. Inset: schematic of the substrate stack configuration.

except that the TM case shows lower reflection at smaller wavelengths, especially in the 600 to 800 nm range. The reflection data for the 833 nm period grating in Fig. 7(b) follow a similar trend as the grating in Fig. 7(a), with the exception that light trapping is only apparent at wavelengths above approximately 710 nm, for both TE and TM polarizations. This wavelength limit is very close to the theoretical lower wavelength threshold for light trapping of 717 nm, which is a function of the grating period D and incidence angle θ_i , according to $\lambda_{\min} = D(1 - \sin \theta_i)$ [5]. This result shows the importance of the appropriate choice of the grating period as one of the main design criteria for diffractive light trapping, as discussed earlier [5]. For the Si film thickness investigated here, a 600 nm period grating provides improved light trapping.

4. Summary and Conclusions

Light trapping in approximately $1.5 \mu\text{m}$ thick c-Si films through diffractive back reflectors, fabricated by nanoimprinting of a dielectric precursor layer, was studied experimentally and theoretically through RCWA simulations. We compared the simulated and experimental hemispherical reflection of grating and flat back reflectors and the extracted wavelength-dependent optical absorption in the Si layer. The polarization-averaged improvement in solar photon absorption, and short-circuit current, through the grating reflector is 8.5%. The degree of improvement decreases with increasing incidence angle, although light trapping is observed in TE and

TM polarization for incidence angles up to 50° to the surface normal. Through RCWA modeling one can attribute this comparatively low degree of light trapping to the low overall diffraction efficiency of the particular grating structure investigated. Future work will focus on the effect of the dielectric grating cladding on the diffraction efficiencies, and on the potential for improvement of diffraction efficiency through modification of grating parameters and of the type and thickness of the dielectric cladding.

This work was supported by the United States Department of Energy (DOE) Photovoltaic Supply Chain and Cross-Cutting Technologies Grant, DE-EE0000586, and matching funds by the Washington Technology Center (Seattle). Work at the National Renewable Energy Laboratory (NREL) was supported by the United States DOE under contract DE-AC36-99GO10337. The authors thank Stephen T. Meyers and Andrew Grenville (both Inpria Corp.) for providing the dielectric precursor solution, Scott T. Dunham (University of Washington) for valuable discussions, Hao-Chih Yuan (NREL) for experimental support, and David Young (NREL) for advice on dehydrogenating and crystallizing the a-Si:H films. Imprinting, metallization, and microscopy were performed at the Washington Technology Center Microfabrication Laboratory and the University of Washington Nanotechnology User Facility, members of the NSF National Nanotechnology Infrastructure Network.

References

1. C. Heine and R. H. Morf, "Submicrometer gratings for solar-energy applications," *Appl. Opt.* **34**, 2476–2482 (1995).
2. C. W. Teplin, D. S. Ginley, and H. M. Branz, "A new approach to thin film crystal silicon on glass: biaxially-textured silicon on foreign template layers," *J. Non-Cryst. Solids* **352**, 984–988 (2006).
3. P. Bermel, C. Luo, L. Zeng, L. C. Kimerling, and J. D. Joannopoulos, "Improving thin-film crystalline silicon solar cell efficiencies with photonic crystals," *Opt. Express* **15**, 16986–17000 (2007).
4. I. Gordon, L. Carmel, D. Van Gestel, G. Beaucarne, and J. Poortmans, "Fabrication and characterization of highly efficient thin-film polycrystalline-silicon solar cells based on aluminium-induced crystallization," *Thin Solid Films* **516**, 6984–6988 (2008).
5. D. N. Weiss, H.-C. Yuan, B. G. Lee, H. M. Branz, S. T. Meyers, A. Grenville, and D. A. Keszler, "Nanoimprinting for diffractive light trapping in solar cells," *J. Vac. Sci. Technol. B* **28**, C6M98 (2010).
6. H. M. Branz, C. W. Teplin, M. J. Romero, I. T. Martin, Q. Wang, K. Alberi, D. L. Young, and P. Stradins, "Hot-wire chemical vapor deposition of epitaxial film crystal silicon for photovoltaics," *Thin Solid Films* **519**, 4545–4550 (2011).
7. C. Eisele, C. E. Nebel, and M. Stutzmann, "Periodic light coupler gratings in amorphous thin film solar cells," *J. Appl. Phys.* **89**, 7722–7726 (2001).
8. H. Stiebig, N. Senoussaoui, T. Brammer, and J. Müller, "The application of grating couplers in thin-film silicon solar cells," *Sol. Energy Mater. Sol. Cells* **90**, 3031–3040 (2006).
9. C. Haase and H. Stiebig, "Thin-film silicon solar cells with efficient periodic light trapping texture," *Appl. Phys. Lett.* **91**, 061116 (2007).

10. H. Sai, Y. Kanamori, K. Arafune, Y. Ohshita, and M. Yamaguchi, "Light trapping effect of submicron surface textures in crystalline Si solar cells," *Prog. Photovoltaics* **15**, 415–423 (2007).
11. H. F. Shih, S. J. Hsieh, and W. Y. Liao, "Improvement of the light-trapping effect using a subwavelength-structured optical disk," *Appl. Opt.* **48**, F49–F54 (2009).
12. P. Sheng, A. N. Bloch, and R. S. Stepleman, "Wavelength-selective absorption enhancement in thin-film solar cells," *Appl. Phys. Lett.* **43**, 579–581 (1983).
13. M. Gale, B. Curtis, H. Kiess, and R. H. Morf, "Design and fabrication of submicron grating structures for light trapping in silicon solar cells," *Proc. SPIE* **1272**, 60–66 (1990).
14. R. H. Morf, "Solar cell," International Patent WO 92/14270 (1992).
15. F. Llopis and I. Tobias, "The role of rear surface in thin silicon solar cells," *Sol. Energy Mater. Sol. Cells* **87**, 481–492 (2005).
16. L. Zeng, Y. Yi, C. Hong, J. Liu, N. Feng, X. Duan, L. C. Kimerling, and B. A. Alamariu, "Efficiency enhancement in Si solar cells by textured photonic crystal back reflector," *Appl. Phys. Lett.* **89**, 111111 (2006).
17. V. E. Ferry, M. A. Verschuuren, H. Li, R. E. I. Schropp, H. A. Atwater, and A. Polman, "Improved red-response in thin film a-Si:H solar cells with soft-imprinted plasmonic back reflectors," *Appl. Phys. Lett.* **95**, 183503 (2009).
18. K. Söderström, F. J. Haug, J. Escarré, O. Cubero, and C. Ballif, "Photocurrent increase in *n-i-p* thin film silicon solar cells by guided mode excitation via grating coupler," *Appl. Phys. Lett.* **96**, 213508 (2010).
19. D. N. Weiss, S. T. Meyers, and D. A. Keszler, "All-inorganic thermal nanoimprint process," *J. Vac. Sci. Technol., B* **28**, 823–828 (2010).
20. D. L. Young, P. Stradins, Y. Q. Xu, L. Gedvilas, B. Reedy, A. H. Mahan, H. M. Branz, Q. Wang, and D. L. Williamson, "Rapid solid-phase crystallization of high-rate, hot-wire chemical-vapor-deposited hydrogenated amorphous silicon," *Appl. Phys. Lett.* **89**, 161910 (2006).
21. S. T. Meyers, Ph. D. thesis (Oregon State University, 2008).
22. D. E. Aspnes, "Optical properties," in *Properties of Crystalline Silicon*, R. Hull, ed. (INSPEC, 1999), pp. 677–696.
23. E. Yablonovitch and G. D. Cody, "Intensity enhancement in textured optical sheets for solar cells," *IEEE Trans. Electron Devices* **29**, 300–305 (1982).
24. National Renewable Energy Laboratory, "Reference solar spectral irradiance: Air Mass 1.5," <http://rredc.nrel.gov/solar/spectra/am1.5/>.
25. H. W. Deckman, C. B. Roxlo, and E. Yablonovitch, "Maximum statistical increase of optical absorption in textured semiconductor films," *Opt. Lett.* **8**, 491–493 (1983).